ISSN:1984-2295

Revista Brasileira de Geografia Física

Homepage:https://periodicos.ufpe.br/revistas/rbgfe

Geotechnologies for the identification of flood-prone areas in the Una River basin, Pernambuco, Brazil[1]

Julyane Silva Mendes Polycarpo[1], Isaque de Souza Mendes [2], Marcus Metri Correa[3], Erivelto Mercante[4], Albert Einstein Spíndola Saraiva de Moura[5], Fernando Cartaxo Rolim Neto[6]

[1] Master's scholarship from the Foundation for the Support of Science and Technology of the State of Pernambuco - FACEPE. Master's student in the Postgraduate Program in Environmental Engineering – Federal Rural University of Pernambuco – UFRPE. R. Dom Manuel de Medeiros, s/n, Dois Irmãos. CEP: 52171-900 - Recife/PE; julyanemendes@gmail.com (autor correspondente). [2] PhD scholarship from the National Council for Scientific and Technological Development - CNPq. PhD student in the Postgraduate Program in Agricultural Engineering at the State University of Western Paraná – UNIOESTE. R. Universitária, 1619 - Universitário Cascavel - PR – Brasil. CEP: 85819-110; isaque.souzamendes11@gmail.com. [3] Professor at the Department of Rural Technology at UFRPE. R. Dom Manuel de Medeiros, s/n, Dois Irmãos. CEP: 52171-900 - Recife/PE; marcus.metri@gmail.com. [4] Professor at the Exact Sciences Center at UNIOESTE. R. Universitária, 1619 - Universitário Cascavel - PR – Brasil. CEP: 85819-110; erivelto.mercante@unioeste.com.br. [5] Professor at the Department of Agronomy at the Federal Institute of Pernambuco – IFPE. Propriedade Terra Preta, S/N, Zona Rural, Vitória de Santo Antão-PE. CEP: 55602-970; aessmoura@yahoo.com.br. [6] Professor at the Department of Rural Technology at UFRPE. R. Dom Manuel de Medeiros, s/n, Dois Irmãos. CEP: 52171-900, Recife/PE; fernandocartaxo@yahoo.com.br.

Artigo recebido em 00/00/0000 e aceito em 00/00/0000

R E S U M O

Climate change has been causing extreme hydrological events, such as floods, to become increasingly frequent. Watersheds may exhibit varying degrees of susceptibility to these events depending on their climatic, hydrological, geological, morphometric, and anthropic characteristics. To identify factors influencing watershed susceptibility to floods, risk indices coupled with geoprocessing tools can be employed. In this context, the present study aimed to analyze the susceptibility to flood occurrence in the Una River watershed, located in the state of Pernambuco, Brazil, through the determination of morphometric parameters. The QGIS software, along with numerical equations, was utilized to determine geometric, drainage, and relief parameters and to characterize each sub-basin of the Una River watershed. The overall analysis revealed that 40% of the total sub-basins exhibit high susceptibility to floods, while 50% have medium susceptibility, and 10% have low susceptibility to floods. Thus, it was found feasible to conduct a geospatial analysis to assess flood risk in watersheds through the analysis of morphometric parameters.

Keywords: geoprocessing, water resources management, natural disaster, inundation, remote sensing.

Geotecnologias para identificação de áreas sujeitas a enchentes na bacia do rio Una, Pernambuco

A B S T R A C T

As alterações climáticas têm ocasionado eventos extremos de natureza hídrica, como as enchentes, cada vez mais frequentes. As bacias hidrográficas podem se apresentar mais suscetíveis à ocorrência desses eventos dependendo de suas características climática, hidrológica, geológica, morfométrica e antrópica. Para identificar os fatores que influenciam a suscetibilidade das bacias à enchentes, podem ser utilizados índices de risco, atrelados a ferramentas do geoprocessamento. Diante disso, o presente trabalho objetivou analisar, através da determinação de parâmetros morfométricos, a suscetibilidade à ocorrência de enchentes da bacia hidrográfica do rio Una, localizada no estado de Pernambuco, Brasil. Utilizou-se o software QGis, além de equações numéricas, para determinar os parâmetros geométricos, de drenagem e de relevo e realizar a caracterização de cada sub-bacia da bacia do rio Una. A análise geral revelou que que 40% do total das sub-bacias possuem alta suscetibilidade à enchentes enquanto 50% das sub-bacias têm susceptibilidade média e 10% têm baixa suscetibilidade a enchentes. Com isso, verificou-se ser possível realizar uma análise geoespacial para avaliar o risco de enchentes em bacias hidrográficas através da análise dos parâmetros morfométricos.

Palavras-chave: geoprocessamento, gestão de recursos hídricos, desastre natural, inundação, sensoriamento remoto.

[1] Extracted from the first author's master's thesis in Environmental Engineering at UFRPE.

Introduction

In coastal regions located between the tropics, meteorological events can lead to the accumulation of water within a watershed. In addition to this, population growth is causing degradation of natural resources, climate changes, and compromising the resilience of the environment. (Jie et al., 2023).

In this sense, the lack of urban planning is one of the factors that make cities and their populations vulnerable and exposed to the risks that urbanization and natural factors may cause (Gonçalves et al., 2022). The improper disposal of waste, construction of irregular housing, emissions of atmospheric pollutants, among others, have been contributing to the worsening of floods and inundations. Additionally, global warming is causing changes in rainfall patterns.

For the Northeast region of Brazil, researchers from the National Institute for Space Research (INPE) predict that global warming is creating a more severe scenario of rainfall, with longer droughts in the semi-arid region and more intense rains along the coastal area. These intensified rains can lead to floods and inundations in major urban centers.

Flash floods occur due to the rapid increase in the water level of river channels, caused, among other factors, by intense precipitation in a short period. Several Brazilian municipalities are located in areas susceptible to floods of this nature, with riverside communities being the most affected as they are situated in natural flood-prone areas along the rivers. (Dias et al., 2021 e Oliveira et al., 2021).

Therefore, floods in urbanized areas are considered an emerging threat, both to the economy and society (Thanvisitthpon et al., 2020; Fang et al., 2023). They represent approximately 50% of all natural disasters and are responsible for economic losses exceeding 40 billion dollars (Wang et al., 2023). From 1990 to 2019, flood-related natural disasters were also responsible for 242,516 deaths and impacted the lives of 3.55 billion people in 168 countries (Liu et al., 2023).

In rural areas, floods cause losses to local economic activities such as agriculture and livestock (Ntim-Amo et al., 2022). Intense precipitation increases surface runoff of rainwater, consequently reducing water infiltration into the soil. This can lead to increased sediment transport, erosion, loss of fertile soil layer, decreased agricultural production, and deterioration of water quality.

The issues caused by floods in the coastal regions of the state of Pernambuco are also exacerbated by the neglect of the public authorities in implementing mitigation measures (Bernardes et al., 2011). The municipality of Água Preta, for example, along with others located in the Una River basin, experienced severe floods in 1995 and 2000, but none compare to the one in 2010 (Throssell, 2010). After this event, the state government of Pernambuco initiated a Reconstruction Operation to relocate some residents living in riverside areas in the cities of Palmares, Água Preta, and Catende (Cavalcante, 2015). However, there are still residents living in these areas, enduring the annual damages caused by floods.

Some researchers conducted an analysis of expenditures related to climate change-related public policies in the state of Pernambuco and concluded that state laws, despite being in force, are often not taken into account as guidelines to be followed by the government in the implementation of its actions, particularly concerning the mitigation and prevention of environmental disasters (Silva et al., 2021).

To prevent or minimize the consequences of these hydrological events, both structural and non-structural measures can be adopted. Among the structural measures are engineering works, such as the construction of dams. As for non-structural measures, actions promoting sustainable watershed management can be implemented, such as reforestation of slopes and the establishment of riparian vegetation, environmental education programs, and the adoption of soil conservation practices like terracing and contour planting. The adoption of these measures requires identifying areas susceptible to flooding in the watershed, which is presumed to be easily identifiable through the morphometric characteristics of the watershed and the creation of thematic maps.

Horton (1945) was a pioneer in relating watershed discharge to stream order, drainage density, stream length ratio, among other parameters. More recently, researchers have sought to establish connections between morphometric characteristics, including geometric, drainage, and relief parameters, along with climatic, hydrological, geological-geomorphological, and anthropic parameters. The objective is to determine the degree of susceptibility of watersheds to floods and inundations. (Marchi et al., 2010; Silva et al., 2022; Sutradhar e Mondal, 2023).

The identification of the sustainability level is important to assist in loss reduction. Consequently, remote sensing tools and geoprocessing have also been employed to determine the susceptibility of watersheds (Abuzied et al., 2016; Santos et al., 2018; Terêncio et al., 2020; Mishra et al., 2023; Singh et al. 2023).

The relationship between various parameters and the susceptibility level of watersheds to floods and inundations provides a systemic view of the subject. The application of geotechnology in the fields of hydrology, geology, and climatology emerges as an important tool to mitigate the damages caused by climate change and extreme hydrological events. Studying local communities, lifestyles, and interactions with the environment reveals the integration of sociology with other disciplines. Furthermore, the research conducted can assist in the development of Public Policies aimed at mitigating the impacts of climate change and extreme events.

In light of the above, the present study aims to conduct a geospatial analysis of the susceptibility to floods in the Una River watershed, located in the southern forest zone of the state of Pernambuco. This analysis will be carried out by examining morphometric characteristics and utilizing remote sensing and geoprocessing tools to assess the risk of floods.

Material and methods

Study area

The Una River watershed (Figure 1), according to the Pernambuco Water and Climate Agency (APAC), covers an area of 6,740.31 km². Out of this total, over 92% is located in the mesoregions of Zona da Mata Sul and Agreste in the state of Pernambuco, and less than 8% in the state of Alagoas. The watershed is situated between the coordinates 08º17'14" and 08º55'28" south latitude and 35º07'48" and 36º42'10" west longitude and is characterized as Hydrological Planning Unit 5 (UP5).

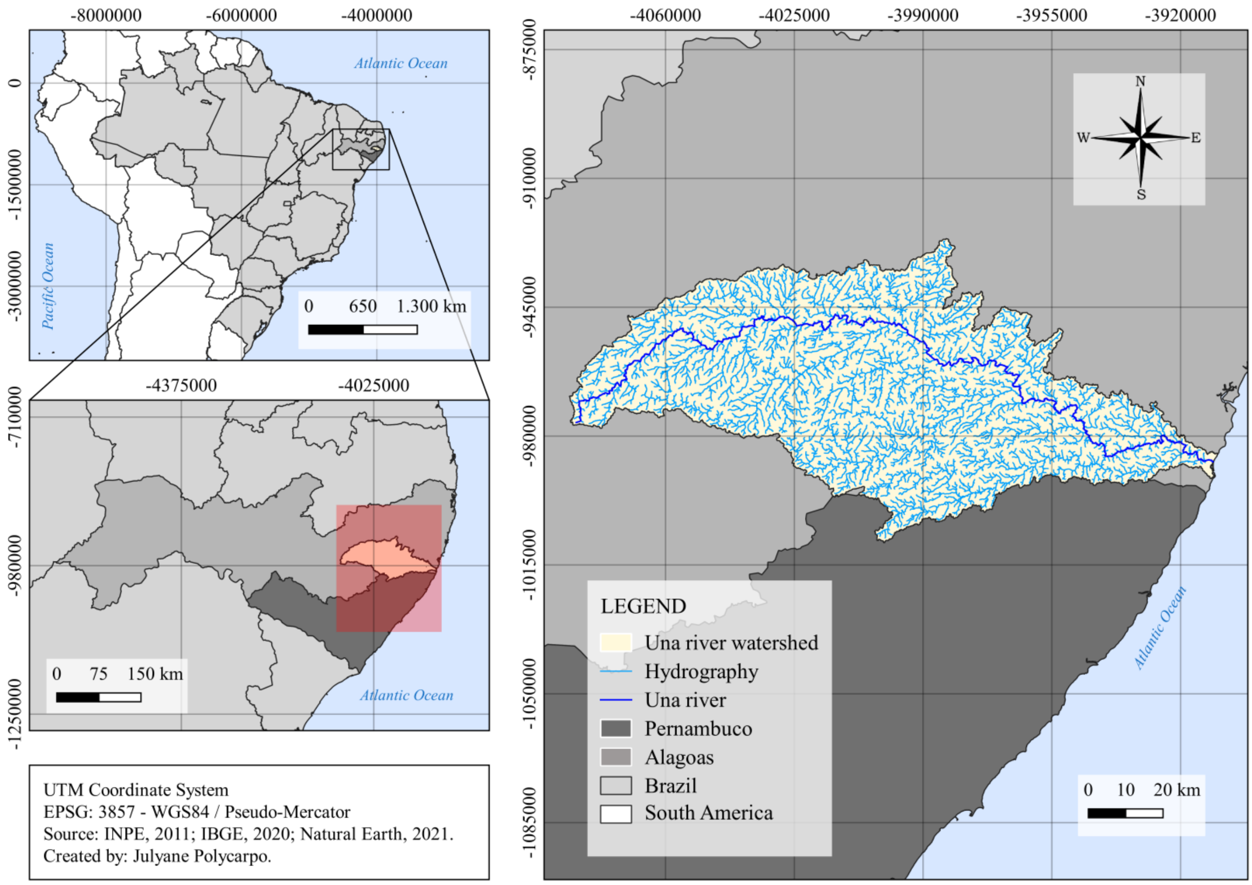

Figure 1. Geographic location of the Una river basin. Source: Authors, 2023.

The Una River originates in the Serra da Boa Vista, in the municipality of Capoeiras, at an altitude of 900m, and flows into the Atlantic Ocean. According to APAC, the river is intermittent until approximately the city of Altinho, becoming perennial afterward. Its main tributaries on the right bank include the Quatis stream, Chata River, Pirangi River, Jacuípe River, and Caraçu River. On the left bank, there are the Riachão stream, Mentirosas stream, Sapo stream, Camevô River, and Preto River.

To the north, the Una River watershed is bordered by the Ipojuca River basin (UP3), Sirinhaém River basin (UP4), and the fourth group of small basins of coastal rivers (GL 4). To the south, it is bordered by the Mundaú River basin (UP6), the state of Alagoas, GL5, and the first group of small basins of inland rivers (GI1). To the east, it is bordered by the Atlantic Ocean, the Sirinhaém River basin, GL4, and GL5. To the west, it is bordered by the Ipojuca and Ipanema River basins (UP7). (APAC, 2022; de-Araujo-Monteiro et al., 2014).

According to the Köppen climate classification, the watershed has a predominantly humid tropical climate with dry seasons during part of the year (Medeiros et al., 2018). The average annual precipitation at different points in the watershed can vary from approximately 300 mm in the west to exceeding 2500 mm in the east (Figures 2 and 3). This difference is primarily caused by the various air currents circulating in the region from the ocean and the southern part of the country, in addition to the influence of the terrain and vegetation.

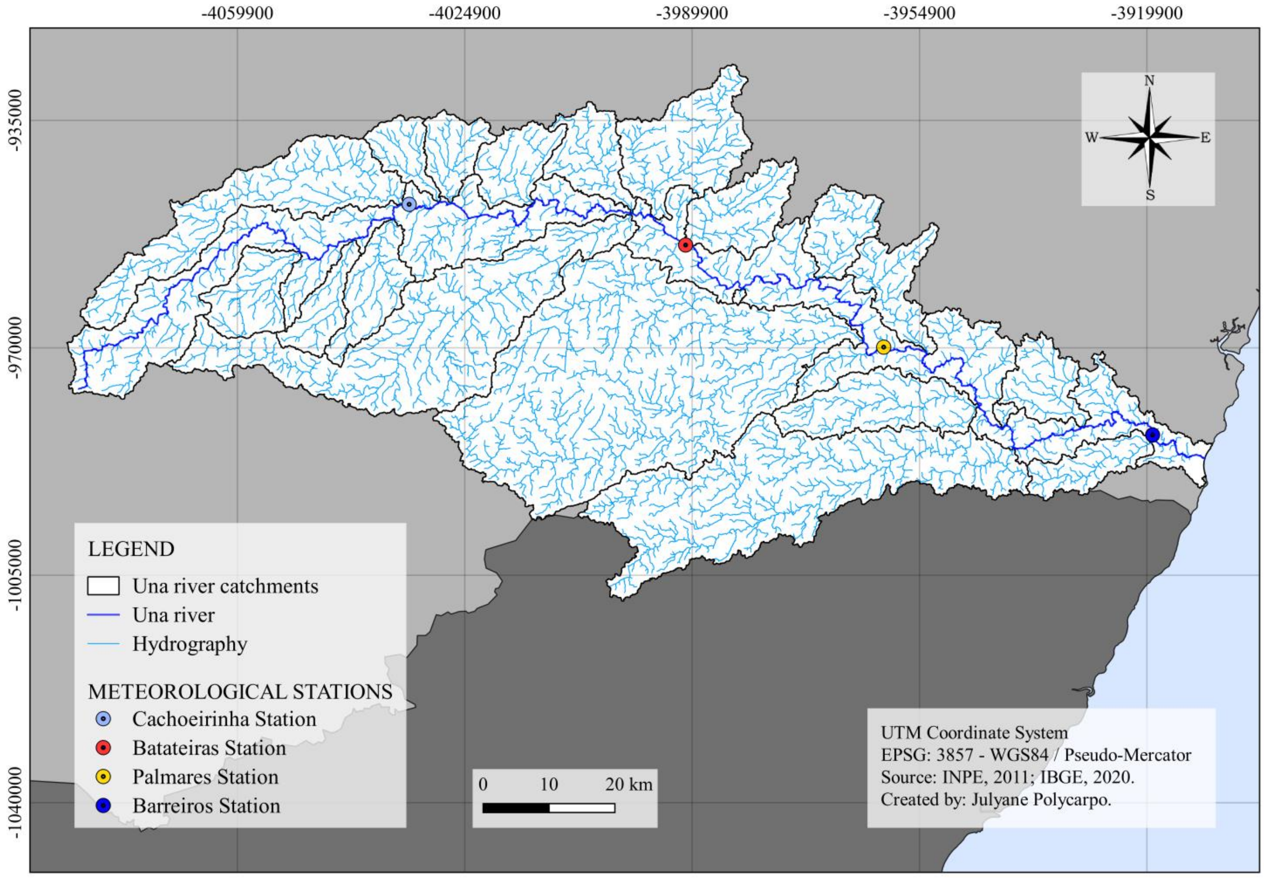

Figure 2. Location of the Cachoeirinha, Batateiras, Palmares and Barreiros meteorological stations. Source:

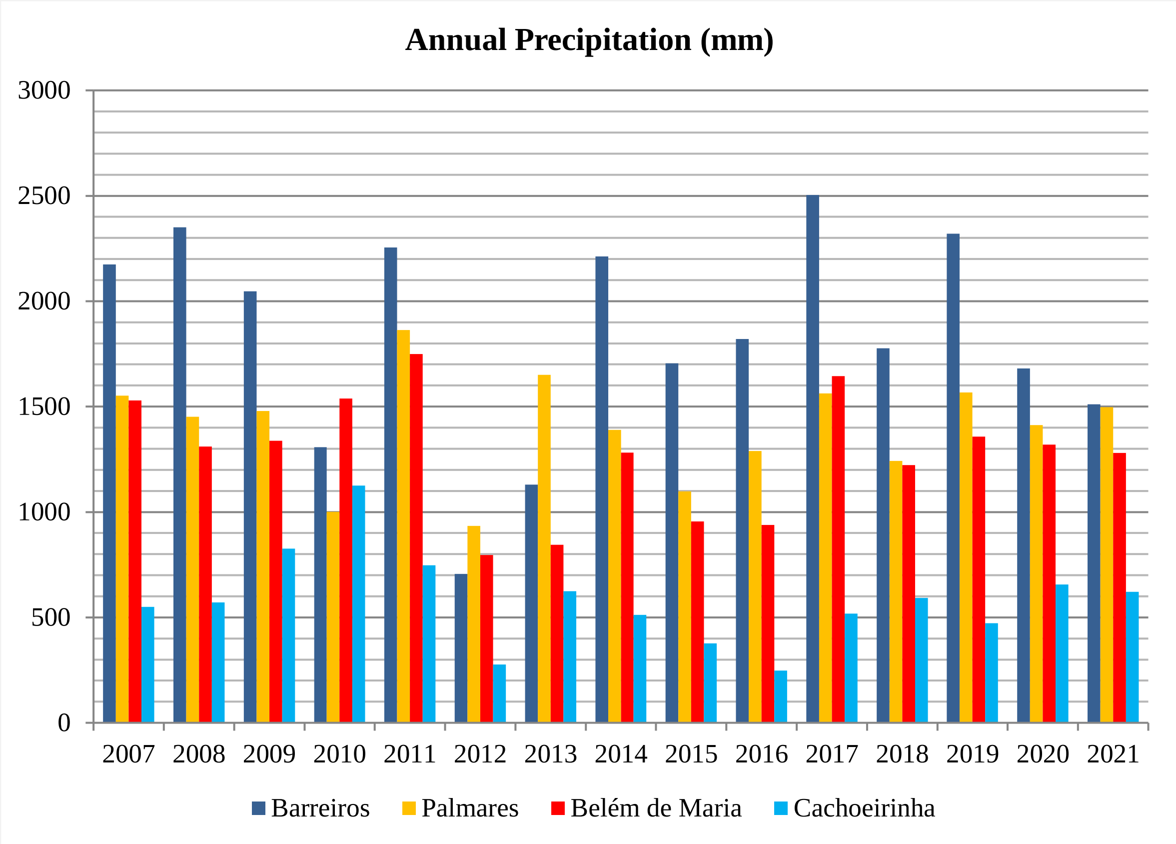

Figura 3. Graph with historical series of annual precipitation (mm) for the cities of Barreiros, Palmares, Belém de Maria and Cachoeirinha. Source: ANA (2022); APAC (2023).

The Una River watershed was chosen as the study area due to the significant flood events recorded in this region in the years 2000, 2005, 2010, 2011, and 2017, causing substantial economic, environmental, social, and even loss of human lives (Melo et al., 2018).

The methodology for acquiring and processing the Digital Elevation Model (DEM), delineation and vectorization of sub-basins and hydrography, as well as the determination of morphometric parameters, was based on Mendes et al. (2016). The methodology for identifying sub-basins was derived from Ogarekpe et al. (2020). The determination of susceptibility level was based on Abuzied et al. (2016).

Four Digital Elevation Models (DEMs) were acquired from the free online Topodata database of the National Institute for Space Research (INPE). The downloaded files were 08S36_ZN, 08S375ZN, 09S36_ZN, and 09S375ZN. According to INPE, these DEMs were generated from data provided by the Shuttle Radar Topography Mission (SRTM) made available by the USGS. The resolution of the DEMs is 30 m..

The processing was carried out in QGIS version 3.16.9, which includes the GRASS 7.8.6 module (QGIS Development Team, 2021). GRASS is necessary as it contains specific tools for hydrological calculations.

The DEMs were merged using the QGIS miscellaneous tool, which can combine the four DEM files. Subsequently, the file was reprojected to the Pseudo-Mercator flat projection (WGS 84 - EPSG: 3857). This system was chosen because the watershed is considered relatively flat, with no significant differences in elevation.

It was necessary to reduce errors in pixel value continuity, i.e., the reduction of spurious depressions in the raster. To achieve this, the DEM underwent a filtering process *(r.fill.dir*), selecting only the "*depression.dem*" function, resulting in a hydrologically consistent DEM (HC-DEM). The HC-DEM was then clipped to reduce processing time in subsequent steps.

Determination of sub-basins, main channel, and hydrography

To initiate the delineation of the Una River watershed and its sub-basins, the HC-DEM underwent processing with the "*r.watershed*" tool, selecting only the "unique label," resulting in a raster of basins.

In the same tool (*r.watershed*), it was necessary to input a minimum normal value (VN), which characterizes a minimum area for a sub-basin to enable the software to carry out the delineation. The VN can be any rounded value or the ratio between the basin area and the resolution area of the DEM. Several values based on the approximate ratio result (value = 7400000) were tested to observe which would provide the best delineation of the watersheds. The VN used for delineation corresponded to 1% of the ratio value, i.e., VN = 74000.

For the vectorization of the raster corresponding to the sub-basins, the "*r.to.vect*" tool was used, selecting the desired layer, feature type (area), and the "*smooth corners of area features*" option, the latter used to smooth the layer edges. This generated a shapefile with the delineated sub-basins. Using the QGIS feature selection tool, only the sub-basins within the Una River basin area were chosen.

To delineate the hydrography, the "*r.watershed*" tool was employed, selecting only the "*stream segments*." It was also necessary to set the minimum normal value, which differed from the one used for basin delineation, as the previous value (VN = 74000) did not provide a significant level of detail for the hydrography. Therefore, for better detailing, VN = 740 was adopted, which is 0.01% of the ratio value between the basin area and the resolution area of the DEM. After this procedure, a raster file for the hydrography was generated.

The vectorization was performed using the "*r.to.vect*" tool, selecting the "*stream segments*" file as the input raster. In this process, the feature type "*line*" was chosen, along with the option "*smooth corners of area features*" to smooth the edges. Finally, the previously generated file was clipped using the Una River basin as the overlay layer.

To identify and quantify the sub-basins within the Una River basin, the methodology of Ogarekpe et al. (2020) was employed. According to the authors, a sub-basin is any set of small basins whose ultimate destination for their water is the main river, in this case, the Una River. Initially, the Una River was selected, and then the set of sub-basins that drain into it was identified. For this, a processing step was performed on the HC-DEM using the "*raster pixels to points*" tool, obtaining elevations for each pixel through a new layer with the values of the centroids of the pixels in the analyzed raster. To identify the main channel, the previously determined hydrography shapefile was used. The source of the Una River was identified as the highest and farthest point from the outlet.

From the identification of the source, it was possible to trace the path taken by the main river by examining the hydrography and elevation values. The river descends to a lower elevation. Then, tributary rivers that flowed to higher elevations were deleted, leaving only the main channel. This allowed observation of which of the small basins discharge into other basins or into the Una River.

Using feature selection tools, vector dissolve, and vector layer merging, it was possible to select the Una River channel. After identifying the main channel bed and using the same tools, several already delineated small basins were merged to form larger sub-basins that discharge into the Una River. After identifying all sub-basins, the hydrography of each sub-basin was delineated using the vector layer clipping tool and their respective main channels.

Morphometric characterization

In the determination of morphometric parameters, the Microsoft Office Excel spreadsheet was used to automate the calculation process. The following parameters were determined for each sub-basin:

a) Geometric parameters

These are the parameters responsible for characterizing the geometry of a hydrographic basin.

Form factor (Ff): is considered the best index to represent the shape of the basin. This parameter indicates that the basin can have high (Ff ≥ 0.75), medium (0.75 > Ff > 0.50), and low (Ff ≤ 0.50) susceptibility to floods (Souza et al., 2017).

$$Ff = \frac{A}{E^2} \tag{1}$$

where Ff – Form factor (dimensionless); A – Basin area (km²); E – Axial length of the basin (km).

The axial length of the hydrographic basin (E) is the distance from the outlet to the furthest point of the basin (km).

Compactness coefficient (Kc): is an index that relates the perimeter of the basin to the perimeter of a circle with the same area as the basin. This parameter indicates that the basin can have high (1.00 < Kc < 1.25), medium (1.25 < Kc < 1.50), and low (Kc > 1.50) susceptibility to floods (Souza et al., 2017).

$$Kc = 0{,}28\frac{P}{\sqrt{A}} \quad (2)$$

where Kc – Compactness coefficient (dimensionless); A – Basin area (km²); P – Basin perimeter (km).

Circularity index (Ic): indicates how closely the shape of the basin approximates a circle. The higher the area, perimeter, and main channel, the greater the likelihood of the basin being elongated. This parameter indicates that the basin can have high (Ic > 0.51), medium (Ic = 0.51), and low (Ic < 0.51) susceptibility to floods (Souza et al., 2017).

$$Ic = 12{,}57\frac{A}{P^2} \quad (3)$$

where Ic – Circularity index (dimensionless); A – Basin area (km²); P – Basin perimeter (km).

b) Drainage parameters

These are parameters that relate to the main metric conditions of the hydrographic network of the basin. This network is a dynamic structure with the capacity to connect the sub-areas that are part of the basin, and by defining a hierarchy of drainage channels, the characteristics of this network can be determined (Vich et al., 2021).

Basin order (O): indicates the degree of branching of the basin. It is chosen so that the tips of the channels, or non-branching channels, are classified as 1st order channels; streams that receive 1st order channels become 2nd order channels; to be 3rd order, the channel needs to receive tributaries of 2nd or 1st and 2nd order (Horton, 1945). The counting continues following the same logic until the main river reaches the mouth, and thus, its order will be the highest and characterizes the order of the basin.

Drainage density (Dd): relates the total length of the drainage channels to the basin area. The higher the Dd, the lower the infiltration capacity (Souza, 2005), and the faster the basin eliminates excess runoff (Vich et al., 2021), thus causing a rapid concentration of floods in flat areas of the basin. This parameter indicates that the basin can have high (Dd > 13.5), medium (5.0 < Dd < 13.5), and low (Dd < 5.0) susceptibility to floods (Strahler, 1952; Souza et al., 2017)

$$Dd = \frac{Lt}{A} \quad (4)$$

where Dd – Drainage density (km/km²); Lt – Total length of drainage channels (km); A – Basin area (km²).

Sinuosity index (Is): a percentage representation between the river and the thalweg (Equation 5). The higher the sinuosity, the greater the susceptibility to floods.

$$Is = 100 * \frac{L - La}{La} \quad (5)$$

c) Relief parameters

Characterizing the relief of a hydrographic basin is important due to its influence on surface runoff, infiltration, water erosion (Vich et al., 2021), and consequently, its impact on the development of floods in the basin.

Average slope of the basin (I): is the tangent of the angle of inclination of the terrain surface along the basin. The slope is inversely proportional to susceptibility to floods, meaning that higher slope results in lower susceptibility. This slope can be determined through the relief amplitude (H) (difference between the maximum and minimum elevations) and the axial length of the basin (Equation 6) (Ávila et al., 2017).

$$I = \frac{Cmáx - Cmín}{E} * 100 = \frac{H}{E} * 100 \quad (6)$$

where I – Average slope of the basin (%); H – Average relief amplitude of the basin (m); E – Axial length of the basin (m).

The classification of the slope can be done according to the Relief Classification determined by Embrapa (1979) (Table 1).

Table 1. Relief classification according to Embrapa.

Relief Classification	Slope (%)
Flat	0 – 3
Gently undulating	3 – 8
Undulating	8 – 20
Strongly undulating	20 – 45
Mountainous	45 – 75
Steep	>75%

Source: Embrapa (1979).

Average slope of the main river (Ieq): It is the ratio between the difference in elevation from the source of the main river to the minimum elevation (outlet) and the length of the main river (Equation 7) (Ávila et al., 2017). Channels with high slopes tend to be smaller and have a greater capacity for erosion and sediment transport (Souza, 2005).

$$Ieq = \frac{Co - Cmín}{L} \quad (7)$$

where Ieq – Slope of the main river (m/m); Co – Elevation of the source of the main river (m); Cmin – Minimum elevation of the basin (m); L – Length of the main river (m).

Concentration time (Tc): It is a parameter influenced by the relief, shape, slope of the basin, soil moisture, among other factors. It can be characterized as the time required for water to travel from the source to the mouth of the main river. Considering the shape of the basins, in elongated basins, tributaries connect to the main river at various points, causing the basin to have a longer concentration time compared to circular basins. Thus, the smaller the concentration time, the more circular the shape of the basin, and the greater its susceptibility to the development of floods (Souza et al., 2017). To determine the concentration time, Equation (8) by Kirpich (1940) can be used.

$$Tc = 57\left(\frac{L^2}{Ieq}\right)^{0,385} \quad (8)$$

where Tc – Concentration time (min); L – Length of the main river (km); Ieq – Slope of the main river (m/km).

Determination of variables

Firstly, all the necessary variables were determined to be used in equations that quantify the geometric, drainage, and relief parameters required for characterizing susceptibility to floods. Variables such as area, perimeter, axial length of the basin and main river, total lengths of drainage channels, length of the main river, basin amplitude, maximum, minimum, average elevations, and the elevation of the source of the main river for all sub-basins were determined.

The area and perimeter were generated using the QGIS field calculator, which has a direct determination for these variables through the Geometry section by selecting "*$area*" and "*$perimeter*" The determined values are in units of "m²" for area and "m" for perimeter.

The variables of axial length of the basin and main river were determined through direct measurement in the *shapefile* using the line measurement tool. For the axial length of the basin, the outlet and the furthest point to it were selected, and for the main river, the outlet was also selected as the starting point, and the source of the main river as the endpoint. The results of the measurements were obtained in "km".

The total length of drainage channels and the main river was determined using the line length sum tool, which generated a new *shapefile*. In the attribute table of the new layer, the sum of the length in "m" was observed. Subsequently, the values were converted to "km".

For the determination of basin amplitude, maximum, minimum, and average elevation, the HC-DEM was used. This *raster* was clipped using the sub-basins as a mask layer, generating new HC-DEM layers for each sub-basin. In each HC-DEM, the QGIS zonal statistics tool was used to calculate selected interval statistics, maximum, minimum, and mean. After processing, a new vector layer was generated containing values for basin amplitude, maximum, minimum, and average elevation in "m," respectively.

Finally, the elevation of the source of the main channel of each sub-basin was determined in "m" using the "raster pixels to points" tool.

To determine the order of each sub-basin, the HC-DEM layers were used. Each *raster* was processed using a tool from the SAGA add-on called "*strahler order*" After processing, another raster file was generated, vectorized, and then classified by categories. Thus, the basin order was identified by the number of categories minus one, as category 1 only identified the base of the raster and was not part of the channel classification.

The average slope of the basin was directly determined using QGIS to obtain more precise results. For this purpose, the HC-DEM was processed using the slope analysis tool, resulting in new *raster* layers of slope. This new layer was processed with the "*zonal statistics*" tool, using the vector file of each basin as the input layer, and the mean was selected as the statistic to be calculated. Consequently, the value of the average slope for each sub-basin was obtained and expressed as a percentage (%). Additionally, the slope raster was reclassified using the “*r.reclass*” tool according to the slope class standards established by Embrapa (1979), as presented in Table 1.

To complement the information, an elevation map of the Una River basin was also generated using the HC-DEM.

Determination of the Flood Susceptibility Index

The susceptibility index for direct analysis parameters, i.e., those for which a higher value indicates a greater tendency of the basin to experience floods, was determined using Equation 9. On the other hand, the determination of the index for inverse analysis parameters, i.e., those for which a lower value indicates a higher susceptibility of the basin to floods, was carried out using Equation 10.

$$Y = \frac{X - Xmín}{Xmáx - Xmín} \quad (9)$$

$$Y = \frac{X - Xmáx}{Xmín - Xmáx} \quad (10)$$

where Y – Degree of flood susceptibility; X – Analyzed parameter (geometric, drainage, and relief); Xmax - Maximum value presented in the evaluated parameter; Xmín - Minimum value presented in the evaluated parameter.

Through the standardization of parameters, the degree of susceptibility (Y) to low, medium, and high flood risk was determined for each sub-basin within the Una River watershed. The susceptibility degree ranges from 0 to 1 and was classified according to the intervals presented below (Table 2).

Table 2. Reference Intervals for Morphometric Susceptibility Degrees

Corresponding Degree	Low	Medium	High
Y	0 – 0.33	0.34 – 0.66	0.65 – 1.0

Similar to the study conducted by Abuzied et al. (2016), in this work, it was also considered that all parameters carry equal weight, meaning they have the same degree of influence on flood susceptibility.

Finally, flood susceptibility maps were created, each influenced by individual morphometric parameters, for a better visualization of the impact of each parameter on flood development in the sub-basins. Additionally, a comprehensive susceptibility map was developed, combining the influence of all parameters through the summation of their respective Y degrees.

Results and discussion

Una River Watershed

The delimited Una River watershed has an area of 6,701.05 km², a perimeter of 788.6958 km², and an axial length of 172.00 km. It also has an amplitude of 1,025.16 m, a maximum elevation of 1,026.94 m, an average elevation of 460.10 m, and a minimum elevation of 1.78 m near the outlet (Figure 4).

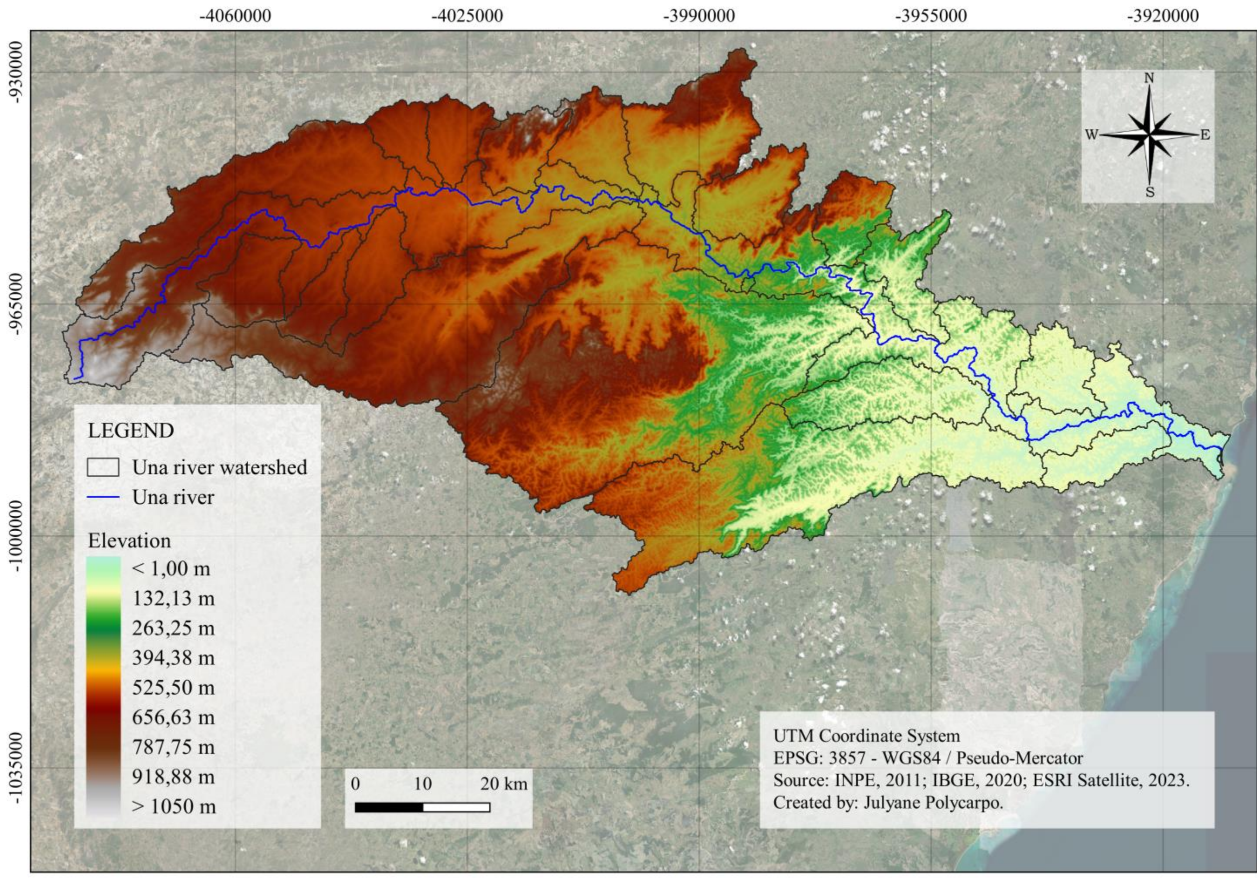

Figure 4. Elevation map of the Una River watershed.

It is a watershed classified as 7th order (Figure 5), with a total length of drainage channels amounting to 5,683.73 km. There is an increase in the number of streams with the rise in order, indicating that the watershed tends to decrease in slope gradient as it approaches the coastal area (Nikhil Raj & Azeez, 2012)

The slope of the watershed, according to Embrapa's classification (1979), can be observed in Figure 6. The Una River watershed has an average slope of 7.66%, featuring a terrain classified as gently undulating, which significantly influences erosive processes during precipitation periods (Leal et al., 2019).

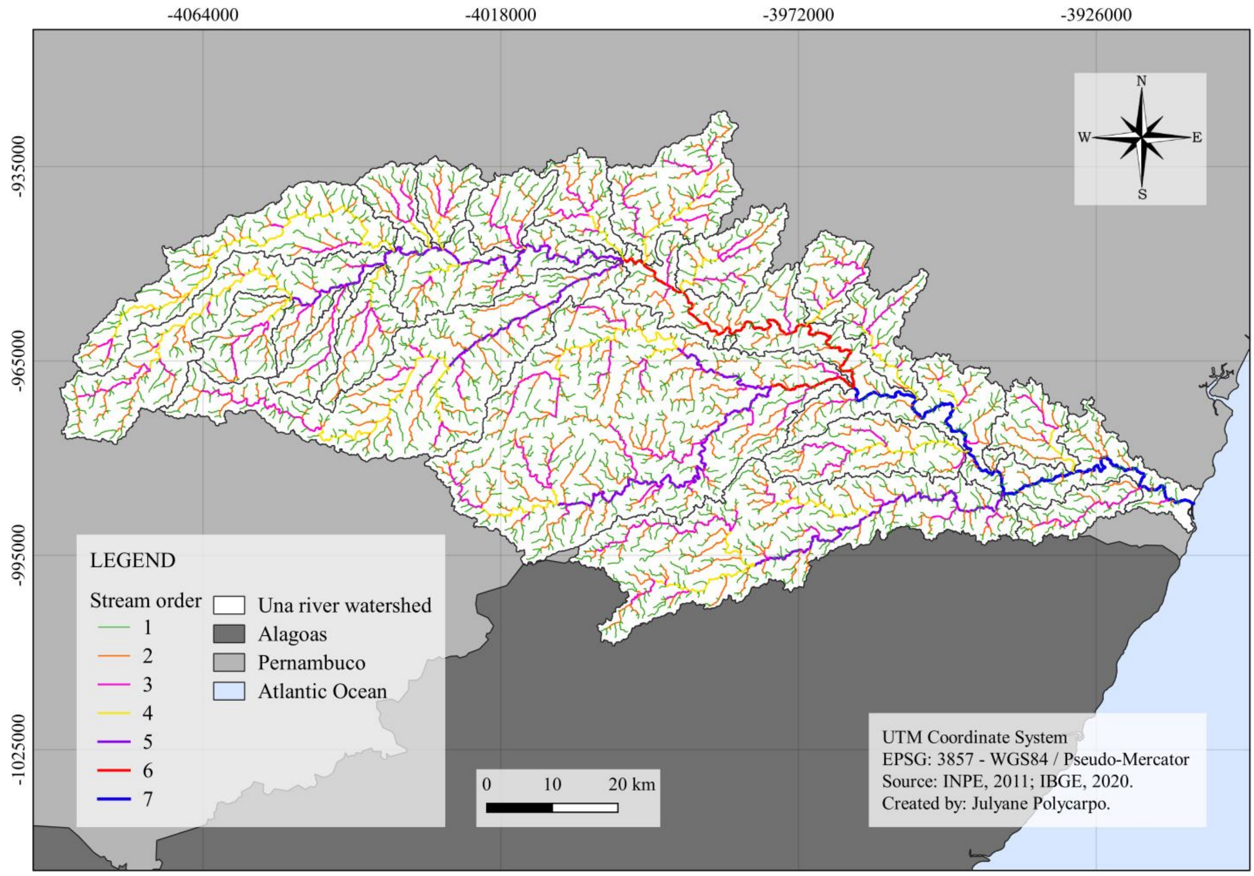

Figure 5. Order of drainage channels in the Una River watershed.

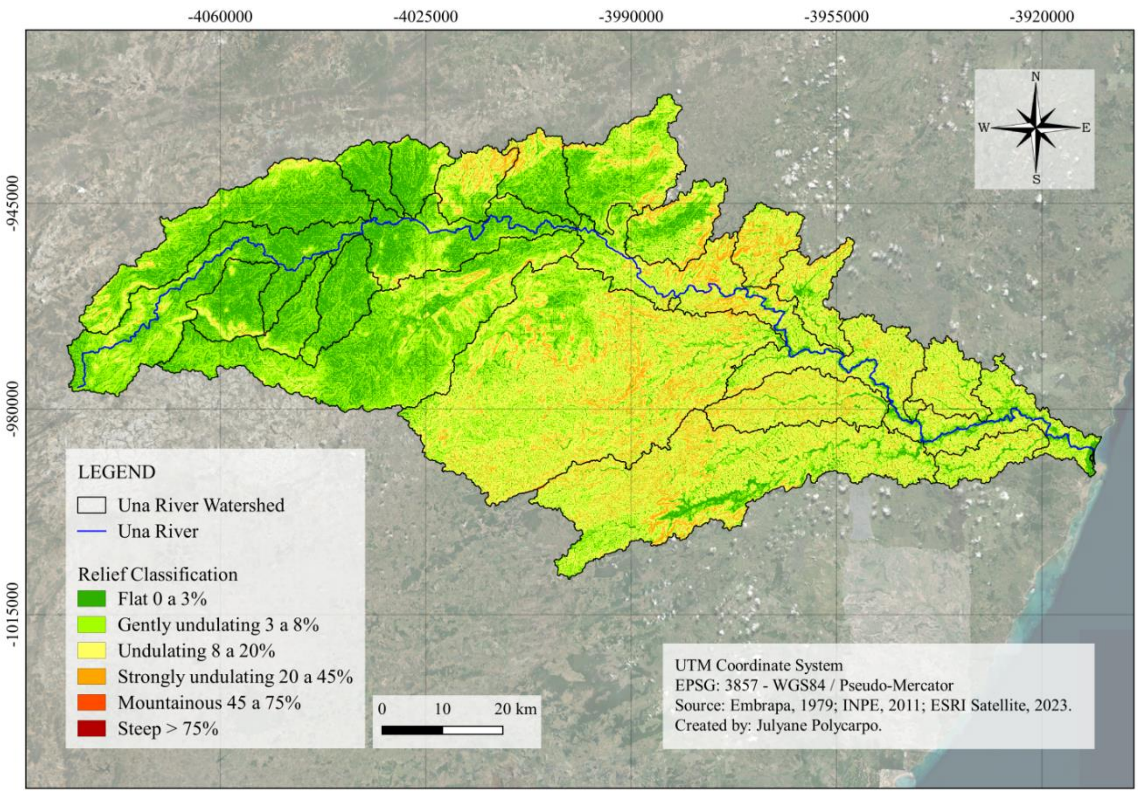

Figure 6. Slope classification of the Una River watershed according to Embrapa (1979).

The main channel of the watershed is the Una River, with a total length of 315.517 km, an axial length of 170.59 km, and its source at an elevation of 936.27 m. Its average slope (3 m/km) indicates that the area drained by this river system naturally does not experience significant pressure from fluvial erosion (Capoane and Silva, 2020). The channel of the watershed has an area of 1,517.98 m² and a perimeter of 890.06 m. The morphometric parameters of the Una River watershed are presented in Table 3.

Table 3. Morphometry of the Una River watershed.

Morphometric Parameters	Geometric Parameters	A (Km²)	6,701.05
		P (Km)	788.70
		E (Km)	172.00
		Ff	0.22
		Kc	2.70
		Ic	0.14
	Drainage Parameters	Order	7.00
		Dd (Km/Km²)	0.85
		Is (%)	84.96
	Relief Parameters	I (%)	7.66
		Ieq (m/m)	0.0030
		Tc (min)	3,151.91
		Tc (hours)	52.53

Source: Authors, 2023.

Legend: A = Area; P = Perimeter; E = Axial length of the watershed; Ff = Form factor; Kc = Compactness coefficient; Ic = Circularity index; O = Order of the watershed; Dd = Drainage density; Is = Sinuosity index; I = Average slope of the watershed; Ieq = Average slope of the main river; Tc = Concentration time.

The form factor closer to zero indicates that the watershed has a more elongated shape, as can be observed in Figure 1, suggesting lower susceptibility to floods. The compactness coefficient (Kc > 1.5) and the circularity index (Ic < 0.51) suggest that the Una River watershed has low susceptibility to floods.

The high order of the watershed and the sinuosity index present elevated values, indicating vulnerability to floods in the Una River watershed. Additionally, the high concentration time, besides indicating that the watershed is more elongated, also suggests low susceptibility to floods.

In general, geometric parameters indicate low susceptibility to floods, while drainage and relief parameters indicate a propensity for floods, as also discussed by Pinto et al. (2016).

Morphometry of sub-basins

The Una River watershed comprises a total of 20 sub-basins (Figure 7).

The variables required for determining the morphometric parameters of each sub-basin are presented in Table 4. Additionally, the morphometric parameters of each sub-basin have also been determined and are presented in Table 5

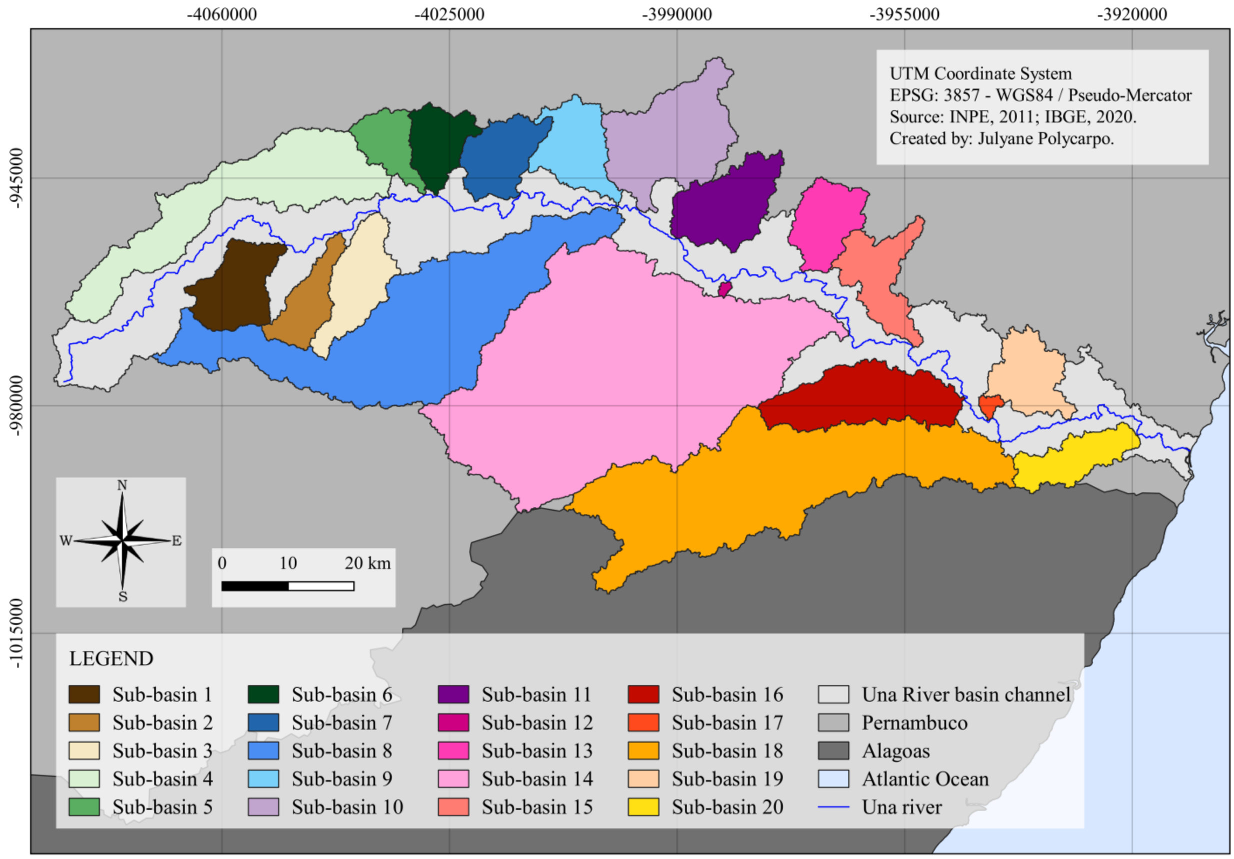

Figure 7. Sub-basins of the Una River watershed.

.

Table 4. Numerical variables of the 20 sub-basins of the Una River.

Sub-basin	Variables										
	A (Km²)	**P (Km)**	**E (Km)**	**La (Km)**	**Lt (Km)**	**L (Km)**	**H (m)**	**Cmáx (m)**	**Cmín (m)**	**Cméd (m)**	**Co (m)**
1	130.05	68.46	17.72	16.54	110.93	27.99	324.74	678.38	570.91	895.64	857.05
2	87.36	66.30	19.53	18.37	66.07	24.78	289.28	838.98	549.71	650.74	767.07
3	134.13	79.21	23.81	22.95	113.03	29.83	257.38	793.73	536.35	608.42	731.35
4	393.00	186.24	51.87	50.56	315.24	83.81	412.09	942.02	529.92	662.30	866.66
5	76.50	57.81	15.23	14.22	66.23	18.06	198.15	719.96	521.81	594.42	634.79
6	90.07	56.64	14.21	11.21	77.74	18.88	312.80	827.06	514.26	591.38	702.25
7	115.05	64.50	12.82	11.36	93.14	17.47	597.61	1,026.94	429.33	623.13	820.97
8	718.17	259.69	74.13	73.07	585.42	114.57	553.35	933.16	379.81	635.28	882.50
9	126.79	81.58	18.82	17.66	110.79	27.91	641.63	1,020.81	379.18	517.13	846.84
10	265.94	110.52	26.21	25.24	233.90	35.69	521.63	886.61	364.98	543.77	749.16
11	154.73	78.12	20.57	16.53	127.12	25.75	497.69	826.33	328.64	474.08	572.28
12	3.21	9.52	2.61	1.52	1.53	1.53	149.88	413.43	281.55	344.83	311.85
13	110.46	61.61	15.69	13.87	95.48	28.36	657.86	803.34	145.49	434.20	624.50
14	1,399.28	256.68	66.48	56.43	1,217.95	92.35	777.39	886.02	108.63	489.66	808.36
15	126.79	97.21	19.87	18.14	110.92	25.73	375.73	468.61	92.88	206.59	319.92
16	217.75	107.49	31.70	30.12	179.99	43.41	392.82	455.97	63.15	169.86	314.84
17	8.66	17.10	3.86	2.15	6.50	4.11	126.23	183.09	56.87	101.94	82.50
18	808.73	274.26	67.02	65.90	718.95	112.34	716.76	769.36	52.60	288.21	582.68
19	115.82	76.77	16.66	14.03	94.88	22.85	170.90	209.85	38.95	112.26	115.00
20	100.59	74.38	20.30	18.02	89.62	27.77	156.99	166.30	9.31	83.36	102.09

Legend: A = Area; P = Perimeter; E = Axial length of the watershed; La = Axial length of the main river; Lt = Total length of drainage channels; L = Length of the main river; H = Average amplitude of the basin; Cmx = Maximum elevation of the basin; Cmin = Minimum elevation; Cavg = Average elevation; Co = Elevation of the source.

Table 5. Morphometric Parameters of Uma River Sub-basins.

Sub-basin	Morphometry												
	Geometric Parameters					Drainage Parameters				Relief Parameters			
	A (Km²)	P (Km)	E (Km)	Ff	Kc	Ic	O	Dd (Km/Km²)	Is (%)	I (%)	Ieq (m/m)	Tc (min)	Tc (hours)
1	130.05	68.46	17.72	0.41	1.68	0.35	4.00	0.85	69.22	18.32	0.01022	302.97	5.05
2	87.36	66.30	19.53	0.23	1.99	0.25	3.00	0.76	34.89	14.81	0.00877	292.52	4.88
3	134.13	79.21	23.81	0.24	1.92	0.27	4.00	0.84	29.97	10.81	0.00654	377.88	6.30
4	393.00	186.24	51.87	0.15	2.63	0.14	4.00	0.80	65.79	7.95	0.00402	1,009.95	16.83
5	76.50	57.81	15.23	0.33	1.85	0.29	4.00	0.87	26.96	13.01	0.00626	261.21	4.35
6	90.07	56.64	14.21	0.45	1.67	0.35	4.00	0.86	68.48	22.02	0.00996	226.03	3.77
7	115.05	64.50	12.82	0.70	1.68	0.35	4.00	0.81	53.87	46.60	0.02241	155.80	2.60
8	718.17	259.69	74.14	0.13	2.71	0.13	5.00	0.82	56.79	7.46	0.00439	1,241.94	20.70
9	126.79	81.58	18.82	0.36	2.03	0.24	4.00	0.87	58.06	34.09	0.01676	249.88	4.16
10	265.94	110.52	26.21	0.39	1.90	0.27	4.00	0.88	41.43	19.90	0.01076	358.12	5.97
11	154.73	78.12	20.57	0.37	1.76	0.32	4.00	0.82	55.78	24.20	0.00946	292.73	4.88
12	3.21	9.52	2.61	0.47	1.49	0.44	1.00	0.48	1.03	57.42	0.01974	25.14	0.42
13	110.46	61.61	15.69	0.45	1.64	0.37	4.00	0.86	104.53	41.92	0.01689	252.28	4.20
14	1,399.28	256.67	66.48	0.32	1.92	0.27	6.00	0.87	63.66	11.69	0.00758	852.44	14.21
15	126.79	97.21	19.87	0.32	2.42	0.17	4.00	0.87	41.85	18.91	0.00882	300.49	5.01
16	217.75	107.49	31.70	0.22	2.04	0.24	4.00	0.83	44.12	12.39	0.00580	528.46	8.81
17	8.66	17.10	3.86	0.58	1.63	0.37	2.00	0.75	90.98	32.69	0.00624	83.54	1.39
18	808.73	274.26	67.02	0.18	2.70	0.14	5.00	0.89	70.47	10.69	0.00074	2,430.78	40.51
19	115.82	76.77	16.66	0.42	2.00	0.25	4.00	0.82	62.83	10.26	0.00333	399.25	6.65
20	100.59	74.38	20.30	0.24	2.08	0.23	3.00	0.89	54.08	7.73	0.00334	463.11	7.72

Legend: A = Area; P = Perimeter; E = Axial length of the watershed; Ff = Form factor; Kc = Compactness coefficient; Ic = Circularity index; O = Order of the watershed; Dd = Drainage density; Is = Sinuosity index; I = Average slope of the watershed; Ieq = Average slope of the main river; Tc = Concentration time.

Sub-basin 12 is the one with the smallest area, presenting the lowest values for almost all parameters, except for the form factor, circularity index, and the average slopes of the watershed and the main river. The smallest form factor value was identified in sub-basin 8 (Chata River basin, Ff = 0.13), followed by sub-basin 18 (Jacuípe River basin, Ff = 0.18), indicating a more elongated shape compared to the others. Additionally, sub-basin 12 had the highest values for circularity indices (Ic = 0.44) and the average slope of the watershed (I = 57.42%), compared to other sub-basins. The lowest value for the average slope of the main river was presented in sub-basin 18 (Ieq = 0.00074 m/m).

Sub-basin 8 had the highest values for axial length of the watershed (E = 74.14 km), compactness index (Kc = 2.71), and circularity index (Ic = 0.13), also presenting the lowest value for the average slope of the watershed (I = 7.46%) when compared to other sub-basins. Sub-basin 7 (Riachão stream basin) had the highest value for the form factor (Ff = 0.70) and the average slope of the main river (Ieq = 0.02241 m/m). Sub-basin 18 had the highest values for perimeter (P = 274.26 km) and concentration time (Tc = 40.51 hours). Sub-basin 14 (Pirangi River basin) had the highest values for area (A = 1,399.28 km²) and order (O = 6.00). Sub-basin 13 (Camevô River basin) had the highest value for sinuosity index (Is = 104.53%).

The drainage density with the highest value was identical for sub-basins 18 and 20 (Dd = 0.89 km/km²). High drainage density values indicate low values for the average slope of the main river, as observed by Saha et al. (2022). The order is directly proportional to the area, cross-sectional area of the stream, and the flow it carries. Therefore, sub-basins with higher order have a larger area, resulting in higher discharge (López-Ramos et al., 2022).

Flood Susceptibility Index

The flood susceptibility index for each morphometric parameter was generated and used to create specific susceptibility maps (Figures 8, 9, and 10). After identifying the influence of each morphometric parameter on flood susceptibility in each sub-basin, the overall susceptibility degree was determined by summing all the specific indices for each sub-basin (Table 6).

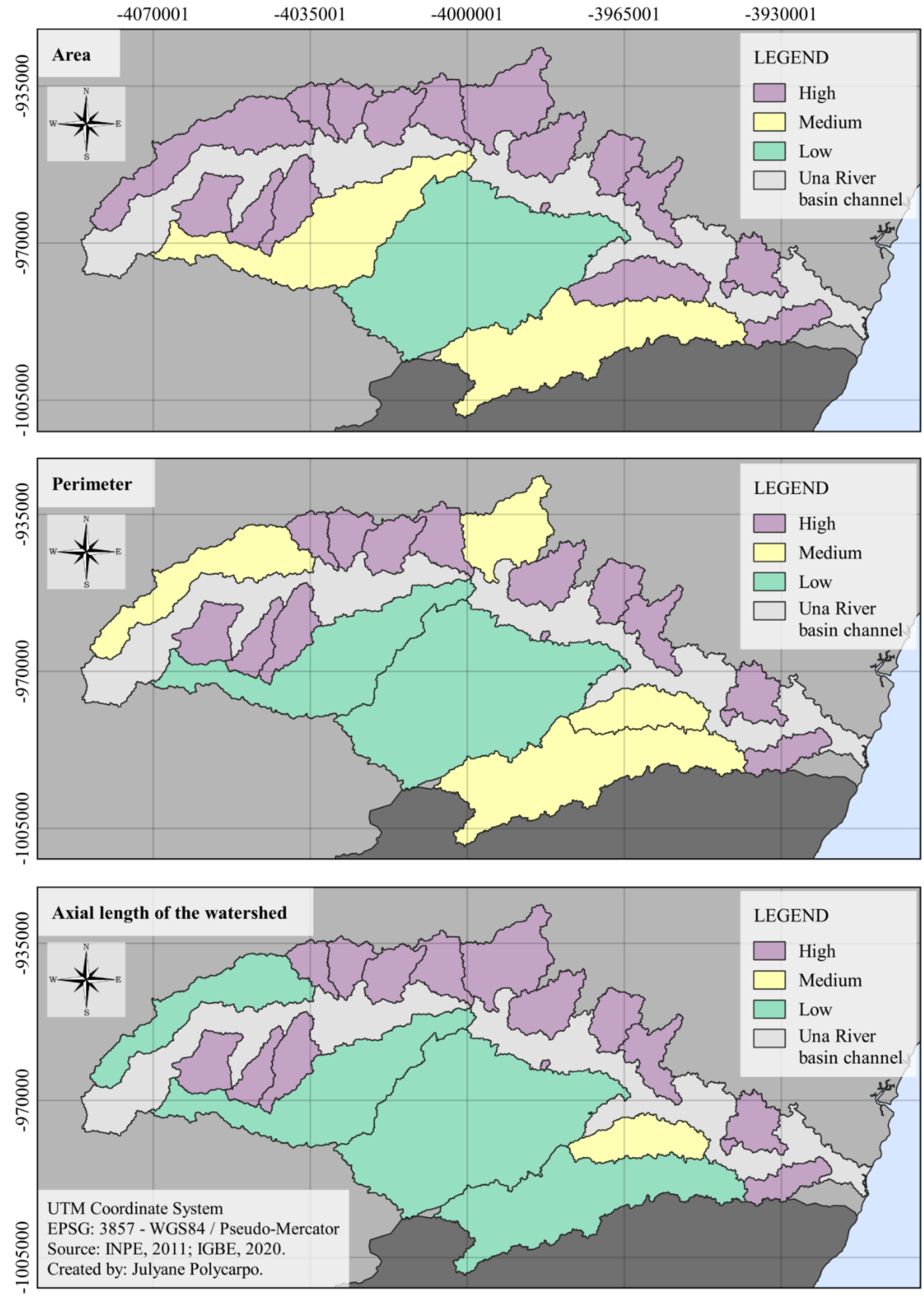

Figure 8.1 Flood susceptibility risk maps according to geometric parameters.

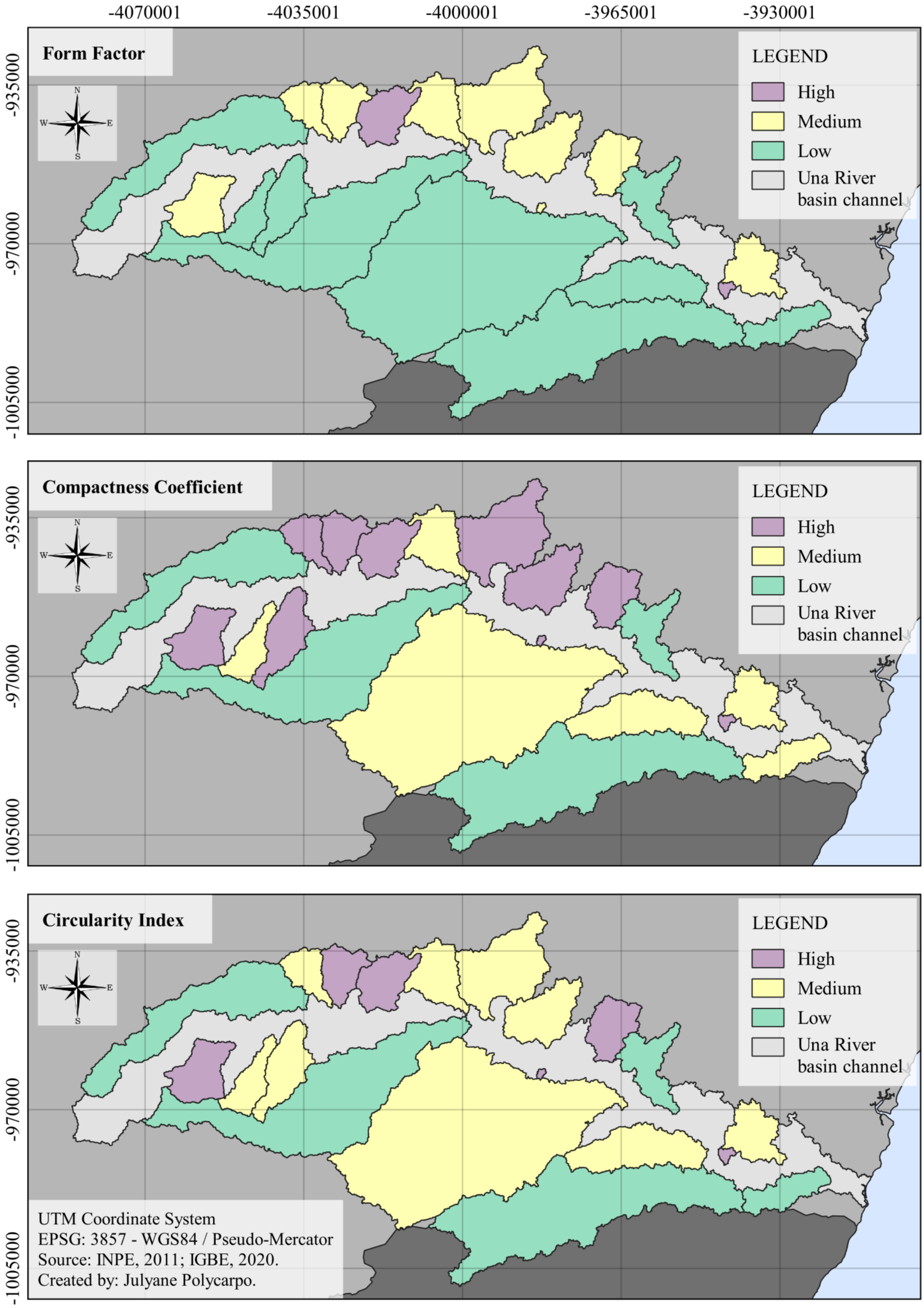

Figure 8.2 Flood susceptibility risk maps according to geometric parameters.

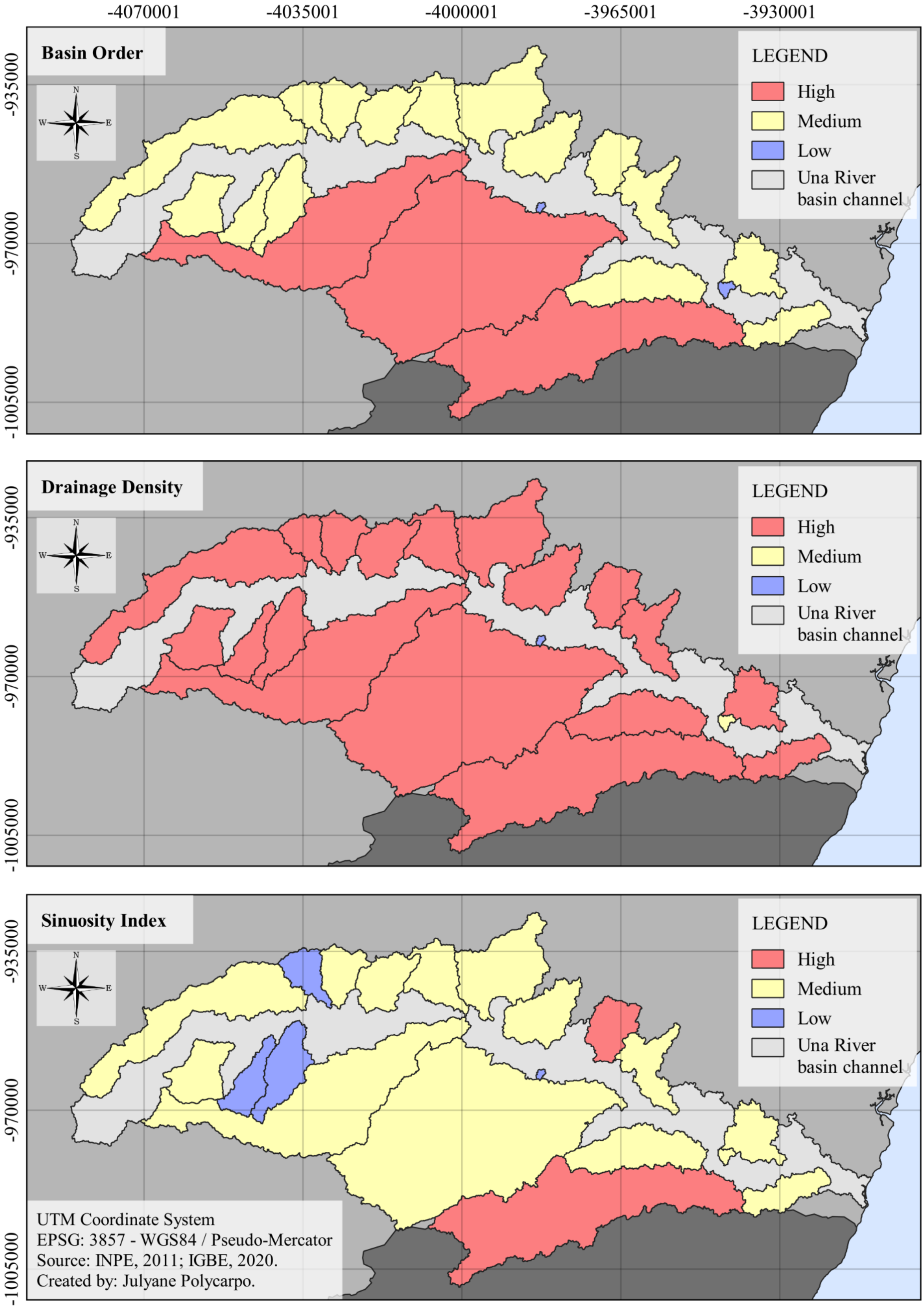

Figure 9. Flood susceptibility risk maps according to drainage parameters.

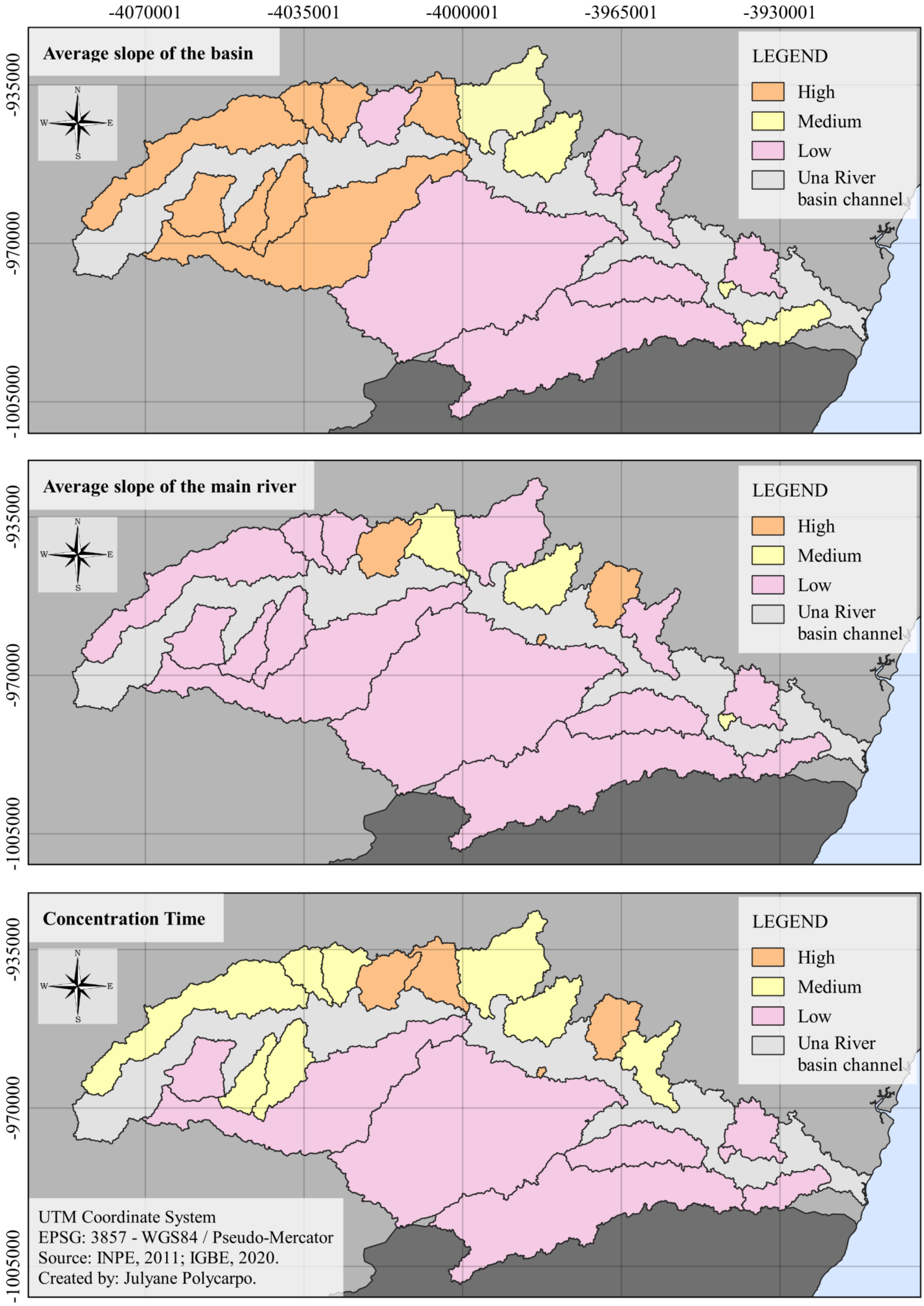

Figure 10. Flood susceptibility risk maps according to relief parameters.

Table 6. Overall Susceptibility Degree of the Uma River Basin.

Sub-basin	Degree
1	8.22
2	6.47
3	6.70
4	4.51
5	7.29
6	8.52
7	9.11
8	3.67
9	7.77
10	6.98
11	7.34
12	7.63
13	8.69
14	4.79
15	5.87
16	5.43
17	8.27
18	3.43
19	6.39
20	5.88

The overall susceptibility degree indicates that 40% of the total sub-basins have a high susceptibility to floods, while 50% of the total sub-basins have a medium probability, and 10% of the total have low susceptibility to floods. Sub-basin 8 has the lowest flood susceptibility index, while sub-basin 7 has the highest index, with values of 2.87 and 8.79, respectively. This information can be better observed on the overall map with the susceptibility degree of the Una River watershed (Figure 11). Thus, similar to the findings by Abuzied et al. (2016) and Singh et al. (2023), using DEM allowed the identification of the sub-basins most susceptible to flooding and the analysis of morphometric parameters influencing this susceptibility.

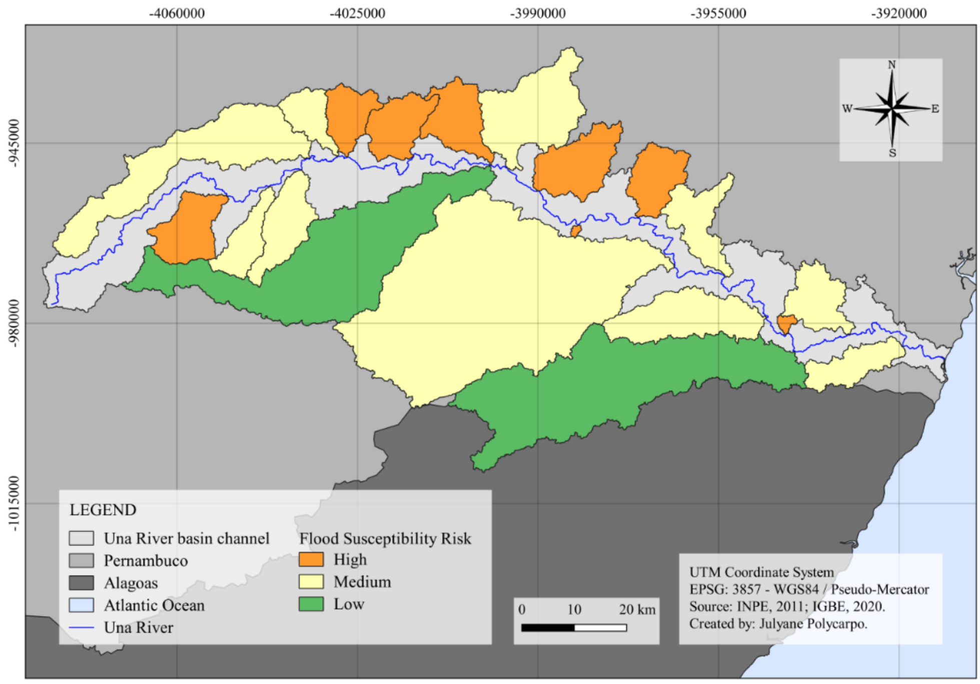

Figure 11. Flood Susceptibility Risk Map of the Una River Basin.

Conclusions

A geospatial analysis of flood susceptibility in the Una River watershed was successfully conducted using a risk index methodology and remote sensing tools.

A detailed analysis of each sub-basin of the Una River was achieved, resulting in a precise risk map.

Sub-basins 1 (Mucambo stream), 6 (Fundo stream), 7 (Riachão stream), 9 (Mentirosas stream), 11 (Prata River), and 13 (Camevô River) showed high susceptibility to floods and should be considered, by the public authorities, as priority sub-basins for actions aimed at erosion and surface runoff control.

Sub-basins 8 (Chata River) and 18 (Jacuípe River) exhibited low susceptibility to floods.

The methodology presented can be applied to any watershed, provided access to Digital Elevation Models and the necessary geoprocessing tools.

Acknowledgments

The first author acknowledges FACEPE for the master's scholarship (IBPG-1626-3.07/19), and the second author acknowledges CNPq for the doctoral scholarship (142151/2020-3). All authors thank the funding agencies mentioned above.

References

Abuzied, S., Yuan, M., Ibrahim, S., Kaiser, M., & Saleem, T. 2016. Geospatial risk assessment of flash floods in Nuweiba area, Egypt. Journal of Arid Environments, 133, 54-72. Available: http://dx.doi.org/10.1016/j.jaridenv.2016.06.004

ANA. Agência Nacional de Águas. HIDROWEB v3.2.6, 2022. Available: <https://www.snirh.gov.br/hidroweb/>. Acesso em 07 mai. 2022

APAC. Agência Pernambucana de Águas e Clima. Bacias Hidrográficas, 2022. Available: <https://www.apac.pe.gov.br/bacias-hidrograficas>. Acesso em: 15 jan. 2023.

APAC. Agência Pernambucana de Águas e Clima. Monitoramento Pluviométrico, 2023. Available: <http://old.apac.pe.gov.br/meteorologia/monitoramento-pluvio.php>. Acesso em: 15 jan. 2023

Ávila, B. T., de Almeida Neto, J. O., & Felippe, M. F. 2017. Suscetibilidade morfométrica a inundações nas bacias hidrográficas tributárias do Rio do Peixe, Zona da Mata de Minas Gerais. Formação (Online), 1(24). Available: https://doi.org/10.33081/formacao.v1i24.4905

Bernardes, D. A. M.; Silva, A. M. & Nascimento, S. S. A história recente das enchentes: a situação das cidades da zona da mata sul de Pernambuco. In: V COLÓQUIO DE HISTÓRIA, Perspectivas históricas – historiografia, pesquisa e patrimônio, Recife. Anais [...]. Recife: Unicap, 2011. p. 1029-1038. Available: <http://www.unicap.br/coloquiodehistoria/wp-content/uploads/2013/11/5Col-p.1029-1038.pdf>. Acesso em: 20 ago. 2020.

Capoane, V. & Silva, D.A. da. 2020. Avaliação de parâmetros geomorfométricos derivados de modelos altimétricos de diferentes fontes e resoluções: estudo de caso da bacia hidrográfica do córrego Lajeado, Campo Grande, MS. Revista Brasileira de Geografia Física, 13(02), 674-690. Available: https://doi.org/10.26848/rbgf.v13.2.p674-690

Cavalcante, P. Em PE, G1 visita Palmares para vero que mudou após enchentes de 2010. Caruaru: G1, 2015. Available: <http://g1.globo.com/pe/caruaru-regiao/noticia/2015/06/em-pe-g1-visita-palmares-para-ver-o-que-mudou-apos-enchentes-de-2010.html>. Acesso em: 20 ago. 2020.

de-Araujo-Monteiro, K., Magalhães-de-Barros, A. C., Tavares-de-Melo, R., Meira-Coelho-Ramos, D. A., Silva-Nóbrega, R., & Girão, O. 2014. Parâmetros morfométricos aplicados à bacia do Rio Una (Pernambuco-Brasil) para identificar susceptibilidade a enchentes. Revista Geográfica De América Central, 1(52), 163-177. Available: https://www.revistas.una.ac.cr/index.php/geografica/article/view/6291

Dias, M.B., Galina, N.R. & Alves, C.N. 2021. Mapeamento da suscetibilidade a inundações em áreas urbanas: estudo de caso no município de Marabá, Sudeste do estado do Pará, Região Norte do Brasil. Revista Ibero-Americana de Ciências Ambientais, 12(6), 347-359. Available: http://doi.org/10.6008/CBPC2179-6858.2021.006.0029

Embrapa. Empresa Brasileira de Pesquisa Agropecuária. Pesquisa do serviço nacional de conservação do solo. Súmula do 10º Encontro de Técnica de Levantamento de Solos. Rio de Janeiro, 1979. 83p.

Fang, X., Zhang, Y., Xiang, Y., Zou, J., Li, X., Hao, C. & Wang, J. 2023. A spatial model for coastal flood susceptibility assessment using the 2D-SPR method with complex network theory: a case study of a reclamation island in Zhoushan, China. Environ. Environmental Impact Assessment Review, 98, 106953, Available: https://doi.org/10.1016/j.eiar.2022.106953.

Gonçalves, E. de O.; Grigio, A.M.; Souza Neto, L.T. de & Diodato, M.A. 2022. Mapeamento da vulnerabilidade socioambiental no espaço urbano de Russas, Ceará, Brasil: Uma integração de dados sociodemográficos e ambientais. Revista Brasileira de Geografia Física, 15(04), 1800-1814. Available: https://doi.org/10.26848/rbgf.v15.4.p1800-1814

Horton, R. E. 1945. Erosional development of streams and their drainage basins; hydrophysical approach to quantitative morphology. Geological society of America bulletin, 56(3), 275-370. Available: https://doi.org/10.1130/0016-7606(1945)56[275:EDOSAT]2.0.CO;2

Jie, H., Khan, I., Alharthi, M., Zafar, M.W. & Saeed, A. 2023. Sustainable energy policy, socio-economic development, and ecological footprint: The economic significance of natural resources, population growth, and industrial development. Utilities Policy, 81, 101490. Available: https://doi.org/10.1016/j.jup.2023.101490

Kirpich, Z. P. 1940. Time of concentration of small agricultural watersheds. Civil Engineering, 10(6), 362.

Leal, J. M., de Aquino, C. M. S., & da Silva, F. J. L. T. 2019. Uso do mapa de Declividade e do Modelo Digital de Elevação na análise do relevo do município de São Miguel do Tapuio–Piauí. Revista de Geociências do Nordeste, 5(2), 97-107. Available: https://doi.org/10.21680/2447-3359.2019v5n2ID18416

Liu, Q.; Yuan, J.; Yan, W.; Liang, W.; Liu, M. & Liu, J. 2023. Association of natural flood disasters with infectious diseases in 168 countries and territories from 1990 to 2019: A worldwide observational study. Global Transitions, 5, 149-159. Available: https://doi.org/10.1016/j.glt.2023.09.001

López-Ramos, A., Medrano-Barboza, J. P., Martínez-Acosta, L., Acuña, G. J., Remolina López, J. F., & López-Lambraño, A. A. 2022. Assessment of Morphometric Parameters as the Basis for Hydrological Inferences in Water Resource Management: A Case Study from the Sinú River Basin in Colombia. ISPRS International Journal of Geo-Information, 11(9), 459. Available: https://doi.org/10.3390/ijgi11090459

Marchi, L., Borga, M., Preciso, E., & Gaume, E. 2010. Characterisation of selected extreme flash floods in Europe and implications for flood risk management. Journal of Hydrology, 394(1-2), 118-133. Available: https://doi.org/10.1016/j.jhydrol.2010.07.017

Medeiros, R. M. de, de Holanda, R. M., & Alexandre, M. 2018. Climate classification in Köppen model for the state of Pernambuco-Brazil. Revista de Geografia (Recife), 35(3). Available: https://doi.org/10.51359/2238-6211.2018.229388

Melo, D. F. B. C. De; Ribeiro, M. H. G.; Albuquerque Junior, E. C. & Gonçalves, E. A. P. 2018. Evaluation of the Una River Basin-Pernambuco: Water Quality Perspective after Construction of 4 Flooding Containment Dams. Revista Brasileira de Geografia Física, 11(2), 612-627. Available: https://doi.org/10.26848/rbgf.v11.2.p612-627

Mendes, I. De. S.; Mercante, E.; Scariotto, M. C.; Maggi, M. F.; Correa, M. M.; Kusminski, D. 2016. Geoprocessing applied to physiographic characterization of the Lontras River Basin-Paraná, Brazil| Geoprocessamento aplicado à caracterização fisiográfica da Bacia do Rio Lontras-Paraná, Brasil. Revista Geama, 2 (3), 249-254. Available: https://www.journals.ufrpe.br/index.php/geama/article/view/872

Mishra, A.K.; Upadhyay, A.; Mishra, P.K.; Srivastava, A. & Rai, S.C. 2023. Evaluating geo-hydrological environs through morphometric aspects using geospatial techniques: A case study of Kashang Khad watershed in the Middle Himalayas, India. Quaternary Science Advances, 11, 100096. Available: https://doi.org/10.1016/j.qsa.2023.100096

Nikhil Raj, P., & Azeez, P. A. 2012. Morphometric Analysis of a Tropical Medium River System: A Case from Bharathapuzha River Southern India. Open Journal of Modern Hydrology, 2(4), 91-98. Available: http://dx.doi.org/10.4236/ojmh.2012.24011

Ntim-Amo, G.; Yin, Q.; Ankrah, E.K.; Liu, Y.; Twumasi, M.A.; Agbenyo, W.; Xu, D.; Ansah, S.; Mazhar, R. & Gamboc, V.K. 2022. Farm households' flood risk perception and adoption of flood disaster adaptation strategies in northern Ghana. International Journal of Disaster Risk Reduction, 80, 103223. Available: https://doi.org/10.1016/j.ijdrr.2022.103223

Ogarekpe, N. M., Obio, E. A., Tenebe, I. T., Emenike, P. C., & Nnaji, C. C. 2020. Flood vulnerability assessment of the upper Cross River basin using morphometric analysis. Geomatics, Natural Hazards and Risk, 11(1), 1378-1403. Available: https://doi.org/10.1016/j.dib.2020.105344

Oliveira, N.R. de, Oliveira Filho, R.A. de, Eleutério, I.A.R. & Oliveira, G.A.G. 2021. Análise da Vulnerabilidade aos alagamentos em canal de escoamento, a partir da simulação de um evento extremo de precipitação, em Montes Claros – Minas Gerais. Revista Brasileira de Climatologia, 28, 544-560. Available: http://dx.doi.org/10.5380/abclima.v28i0.73579

Pinto, V. G., Lima, R. N. D. S., Santos, R. C. P., & Ribeiro, C. B. D. M. 2016. Influência do número de classes de vulnerabilidade na determinação da suscetibilidade morfométrica à inundação. Revista Ambiente & Água, 11, 637-649. Available: http://dx.doi.org/10.4136/1980-993X

Saha, S., Das, J., & Mandal, T. 2022. Investigation of the watershed hydro-morphologic characteristics through the morphometric analysis: a study on Rayeng basin in Darjeeling Himalaya. Environmental Challenges, 7, 100463. Available: https://doi.org/10.1016/j.envc.2022.100463

Santos, C. L.; Silva, O. G.; Vital, S. R. O.; Wanderley, L. S. A. 2018. Análise da

Suscetibilidade à Ocorrência de Enchentes e Inundações na Bacia do Rio Jaguaribe-João Pessoa/PB. Revista Brasileira de Geografia Física, 11(5), 1876-1888. Available: https://doi.org/10.26848/rbgf.v11.5.p1876-1888

Silva, C. E. M. da; Crispim, F. P. & Santos, P. C. B. V. dos. 2021. Revisão Institucional e dos Gastos Públicos no Enfrentamento às Mudanças Climáticas no Estado de Pernambuco. Revista Brasileira de Meio Ambiente, 9 (2), 058-075. Available: https://doi.org/10.5281/zenodo.5550850

Silva, R.C.F. da; Pimentel, M.A. de S. & Araújo, A.N. 2022. Caracterização Morfométrica e Geomorfológica da Bacia Hidrográfica do Rio Itacaiunas (BHRI), Amazônia Oriental, Brasil. Revista Brasileira de Geografia Física, 15(3), 1556-1563. Available: https://doi.org/10.26848/rbgf.v15.3.p1556-1563

Singh, D.; Karan, K.; Singh, S.K.; Chauhan, P. & Berndtsson, R. 2023. Fusing morphometric characteristics with extreme precipitation indices for identifying the most vulnerable sub-basin at risk of flooding. Journal of Hydro-environment Research, 50, 44-56. Available: https://doi.org/10.1016/j.jher.2023.07.005

Souza, C. R. G. 2005. Suscetibilidade morfométrica de bacias de drenagem ao desenvolvimento de inundações em áreas costeiras. Revista Brasileira de Geomorfologia, 6(1). Available: http://dx.doi.org/10.20502/rbg.v6i1.38

Souza, C. F., Pertille, C. T., Corrêa, B. J. S., & Vieira, F. S. 2017. Caracterização morfométrica da bacia hidrográfica do rio Ivaí-Paraná. Geoambiente On-Line, (29). Available: https://doi.org/10.5216/revgeoamb.v0i29.50602

Strahler, A. N. 1952. Dynamic basis of geomorphology. Geological Society of American Bulletin, 63(9), 923-938. Available: https://doi.org/10.1130/0016-7606(1952)63[923:DBOG]2.0.CO;2

Sutradhar, S. & Mondal, P. 2023. Prioritization of watersheds based on morphometric assessment in relation to flood management: A case study of Ajay river basin, Eastern India. Watershed Ecology and the Environment, 5, 1-11. Available: https://doi.org/10.1016/j.wsee.2022.11.011

Terêncio, D. P. S.; Sanches Fernandes, L. F.; Cortes, R. M. V.; Moura, J. P. & Pacheco, F. A. L. 2020. Flood risk attenuation in critical zones of continental Portugal using sustainable detention basins. Science of Total Environment, 721, 137727. Available: https://doi.org/10.1016/j.scitotenv.2020.137727

Thanvisitthpon, N., Shrestha, S., Pal, I., Ninsawat, S. & Chaowiwat, W. 2020. Assessment of flood adaptive capacity of urban areas in Thailand. Environmental Impact Assessment Review,81,106363. Available: https://doi.org/10.1016/j.eiar.2019.106363.

Throssell, L. Atingidos por enchentes em PE moram desde junho em hospital. Brasília: BBC, 2010. Available: <https://www.bbc.com/portuguese/noticias/2010/10/101023_pernambuco_enchente_rp.shtml>. Acesso em: 20 ago. 2020.

Vich, A. I.; Pasquali, E. L. V.; Otta, S. A.; Lauro, C., & Bastidas, L. B. 2021 Morphometric analysis of basins located in the piedmont of central western Argentina. Cuadernos Geográficos, 60(1), 295-312. Available: http://dx.doi.org/10.30827/cuadgeo.v60i1.9639

Wang, Z.; Zhang, F.; Liu, S. & Xu, D. 2023. Consistency between the subjective and objective flood risk and willingness to purchase natural disaster insurance among farmers: Evidence from rural areas in Southwest China. Environmental Impact Assessment Review, 102, 107201. Available: https://doi.org/10.1016/j.eiar.2023.107201